ASSESSMENT OF HIGH-VOLTAGE PHOTOVOLTAIC TECHNOLOGIES FOR THE DESIGN OF A DIRECT DRIVE HALL EFFECT THRUSTER SOLAR ARRAY*

I.G. Mikellides
G.A. Jongeward
Science Applications International Corporation
10260 Campus Point Drive, San Diego, CA 92121

T. Schneider
M.R. Carruth
NASA Marshall Space Flight Center

T. Peterson
T.W. Kerslake
D. Snyder
D. Ferguson
NASA Glenn Research Center at Lewis Field

A. Hoskins
Aerojet Corporation

Abstract

A three-year program to develop a Direct Drive Hall-Effect Thruster system (D2HET) begun in 2001 as part of the NASA Advanced Cross-Enterprise Technology Development initiative. The system, which is expected to reduce significantly the power processing, complexity, weight, and cost over conventional low-voltage systems, will employ solar arrays that operate at voltages higher than (or equal to) 300 V. The lessons learned from the development of the technology also promise to become a stepping-stone for the production of the next generation of power systems employing high voltage solar arrays. This paper summarizes the results from experiments conducted mainly at the NASA Marshal Space Flight Center with two main solar array technologies. The experiments focused on electron collection and arcing studies, when the solar cells operated at high voltages. The tests utilized small coupons representative of each solar array technology. A hollow cathode was used to emulate parts of the induced environment on the solar arrays, mostly the low-energy charge-exchange plasma (10^{12}-10^{13} m^{-3} and 0.5-1 eV). Results and conclusions from modeling of electron collection are also summarized. The observations from the total effort are used to propose a preliminary, new solar array design for 2 kW and 30-40 kW class, deep space missions that may employ a single or a cluster of Hall-Effect thrusters.

Introduction

Electric propulsion, with its highly efficient use of propellant, has long been recognized as the technology of choice for a number of space missions. These include long duration deep space

* Major portions of this paper have been presented at the AIAA 39th Joint Propulsion Conference (Paper no. 2003-4725)

missions as well as station keeping for geostationary satellites. Since its conception over three decades ago the Hall thruster's unique combination of high specific impulse and thrust-to-power ratio established it as a favored propulsion system for a variety of such missions. Employment of these thrusters continues to be evaluated, worldwide, for orbit insertion to LEO,[1] GEO station-keeping,[2] and in more ambitious missions for the human exploration and development of space.[3] A promising systems approach that may significantly reduce cost and weight associated with the employment of these thrusters onboard both deep space and near-Earth spacecraft is the use of direct drive. A joined NASA/Naval Research Laboratory effort conducted in the late 90s demonstrated that direct drive operation with a Hall thruster is indeed a viable option.[4]

In a conventional electric propulsion system, power is supplied by low voltage solar arrays (usually <150 V). The high voltages needed to operate the electric thruster are provided by the (propulsion) power processing unit (PPU). If the array could provide the required voltage directly, the power processing electronics and heat rejection system would be smaller and lighter. The reductions would translate directly into cost savings and/or allow for additional payload. The effort presented here is part of a NASA program that aims to demonstrate this promise for HET applications.

A main focus in the D2HET program has been the assessment of the interactions between high-voltage solar array technologies and the HET-induced environment. Such tests are expected to benefit not only direct drive systems but other high-voltage space applications as well, such as MW-level electric propulsion power systems[5] and the Space Solar Power (SSP) satellite technology.[6] For D2HET, the assessments have been carried out largely through experiments at the NASA Marshal Space Flight Center (MSFC). Wherever possible the experiments have also been supported by modeling and simulation. The plasma environment under which representative solar array coupons have been tested emulates typical conditions under which the flight D2HET solar arrays would be exposed during thruster operation. Such conditions were defined by modeling and simulation calculations that were carried out early in the program.[7] The calculations assumed a representative 2x2 matrix of thrusters and mission scenarios. Specifically the matrix consisted of the 4-kW class Busek-Primex Thruster (BPT4000) and the 1.4-kW Stationary Plasma Thruster (SPT-100), onboard the DS-1 and EXPRESS spacecraft. As an example of the calculations performed to define the induced environment around the solar arrays, Figure 1 shows the computed plume from the BPT-4000. A system study was also conducted by Aerojet to quantify the potential savings of a direct drive system over conventional technologies, and to identify trends that may offer additional benefits at power levels and/or mission scenarios other than the representative 2x2 matrix considered in the D2HET program.[8,9]

The high-voltage assessment tests have been driven by two main plasma interactions concerns: leakage (or "parasitic") currents and arcing. The first will reduce solar array performance, which can in turn affect the overall S/C design if the collected electron current is a significant fraction (more than a few percent) of the current generated by the array. At the higher operating voltages enhanced parasitic currents can easily occur when dielectric surfaces "snap over". Commonly termed "snapover," the phenomenon is the "shift" in the mechanism by which a dielectric achieves current balance, from repelling most of the incoming electrons to emitting secondary electrons. These secondary electrons are emitted as a result of primary electron bombardment of the dielectric surface and get collected by the nearby conductor (which is

usually positively biased), leading to a sudden increase in both current collection and dielectric potential.

Arcing is most prominent when the conducting surfaces, such as exposed interconnects or semiconductor edges, are at a negative potential with respect to nearby insulating surfaces (e.g. when the HET is not operating). If sustained for long periods of time, arcs can lead to permanent electrical shorts. Most of the efforts to investigate the causes of these and other array failures[10,11] have concentrated at voltages greater than -300 V (i.e. lower in magnitude than |-300 V|).

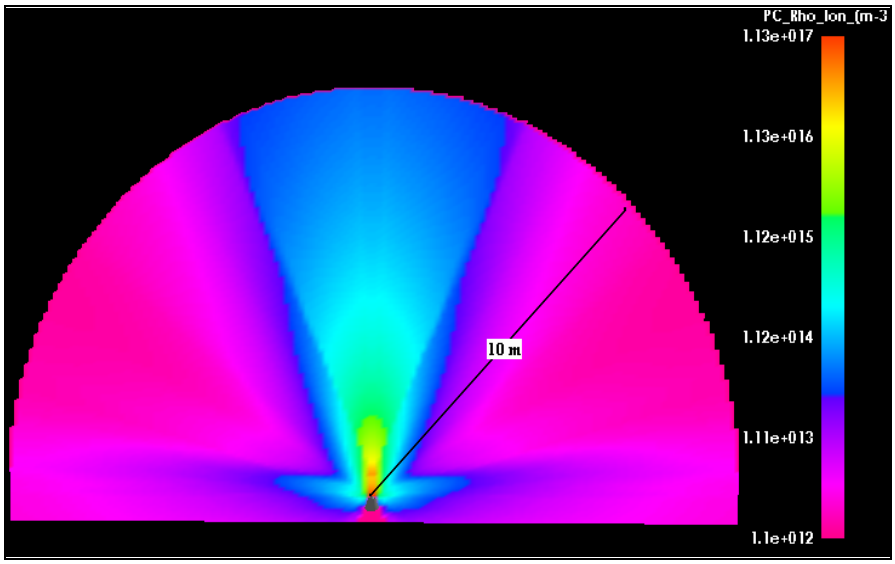

Figure 1. Simulated plume of the BPT-4000 operating at 3 kW showing ion particle density(m^{-3}) within a 10-m radius of the thruster exit.

Solar Array Photovoltaic Technologies

A variety of solar array technologies have been considered some of which employ interconnect shielding from the plasma, array string layout patterns, spacing and grouting, isolation diodes, substrate structural makeup and multi-layer insulation (MLI). We describe below the two main technologies that have been tested at NASA MSFC.

International Space Station (ISS) sample coupon

Several of the technology characteristics mentioned above apply to the ISS solar array. Despite its lower efficiency compared to newer, multi-junction designs such as that by TECSTAR, the ISS design was chosen as a D2HET candidate due to its relative maturity and demonstrated operation in space. Moreover, both on orbit observations and modeling of ISS cells operating at voltages less than 150 V, suggested that the gap geometry shields the exposed semiconductor edges from the plasma and may therefore offer a natural isolation from the environment. No such shielding however has been confirmed at the higher voltages (>300 V) of interest here, where snapover of insulating surfaces is expected to in fact suppress any electric potential barriers and enhance electron current collection.

Two ISS coupons were tested at NASA MSFC one of which is shown in Figure 2. The 15-cell coupon was part of an 80-cell panel (16 x 5 cells) fabricated in 1994 by Lockheed-Martin (Sunnyvale, CA) for the International Space Station Phase 01 Mir Cooperative Solar Array Program. The solar cells were fabricated by SpectroLab, Inc. (Sylmar, CA). The second coupon, cut out of the same 80-cell panel, was identical in geometry to the first coupon. The panel design, materials and fabrication techniques are also identical to those used in the International Space Station Photovoltaic Power Module with two exceptions: (1) the solar cell submodule is 2 x 5 cells (instead of 2 x 4) and (2) the introduction of a pair of small diameter "button holes" in the substrate between solar cells. The latter feature was used to attach the solar cell panels to Russian-built solar array frames. The coupon positive polarity tab (shown to come off cell 56 in Figure 2,a) is connected to the cell p contacts while the negative polarity tab (off of cell 70 in Figure 2,a) is connected to the cell n contacts. A by-pass diode is connected between cells 70 and 61. Figure 2,b shows a top view photograph of the coupon.

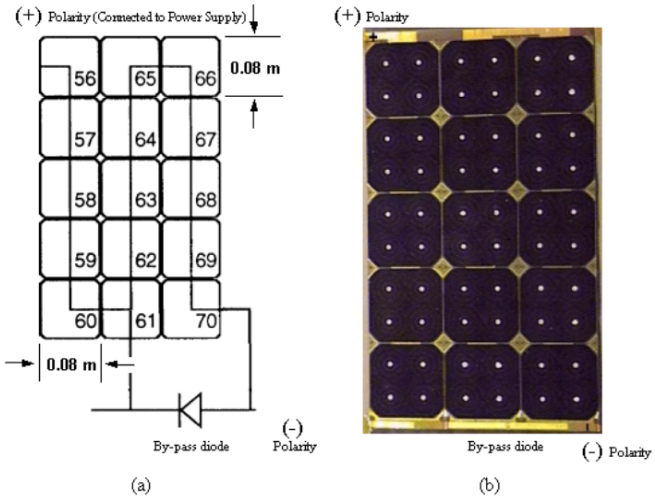

Figure 2. The ISS sample coupon used for the high-voltage D2HET tests.

TECSTAR sample coupon

The TECSTAR coupon is shown in Figure 3. It is comprised of two Solar Power Modules (SPM), each containing two solar cells as shown on the right of Figure 3. The TECSTAR cell is made of Gallium Indium Phosphide/Gallium Arsenide (GaInP/GaAs) on a Germanium (Ge) substrate (active junction). This technology was chosen primarily due to its higher efficiency (GaInP/GaAs/Ge cells have reportedly demonstrated >30% efficiency under concentrated light[12]). In contrast to the ISS coupon the TECSTAR coupon utilizes conventional interconnects that may lead to greater electron collection. The exposed interconnects also increase the possibility of arcing. However, a SPM covers multiple cells with a coverglass. The coverglass isolates interior interconnects from the plasma almost completely but leaves some of the ones that lie around edges partially exposed. To emulate this arrangement in the laboratory Kapton tape was placed on top of part of the edge interconnects (circled as "E" in Figure 3) leaving approximately half of their area exposed. Also in contrast to the ISS coupon, the coverglass does not extend over the solar cell in the direction of the adjacent SPM thus leaving no "overhang".

The coverglass material is made of silica micro sheet and is bonded to the cell with silicon adhesive. The substrate materials consist of Kapton tape laid on top of graphite layer.

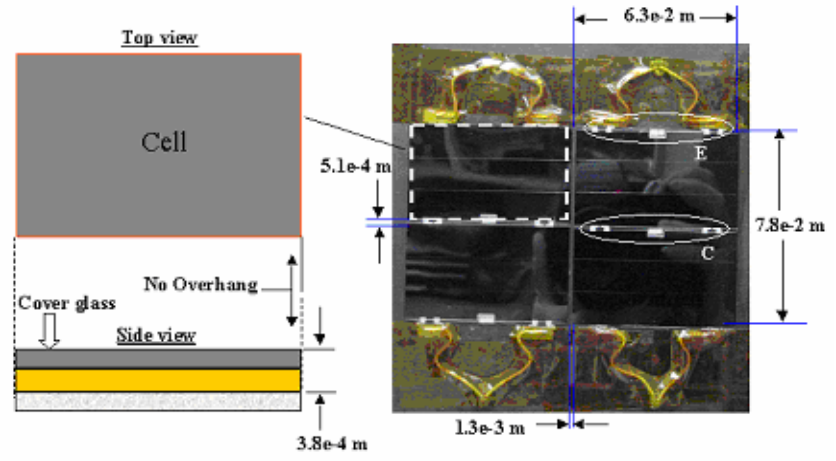

Figure 3. The TECSTAR sample coupon used for the high-voltage D2HET tests.

Facilities

Two vacuum chambers at MSFC were utilized for the tests. Chamber 4605 depicting the ISS solar array sample coupon is shown in Figure 4, left. Chamber 4711 with the TECSTAR coupon is shown in Figure 4, right. The first chamber is approximately 1 meter in diameter and 2 meters long. Two liquid nitrogen trapped diffusion pumps provide the vacuum. A hollow cathode with an annular keeper electrode has been used to simulate the HET plasma conditions in the vacuum chamber. The source was constructed was operated with Argon. The second chamber is of similar dimensions and capabilities, and was used later in the D2HET program for both electron collection and arcing tests.

Plasma particle densities in the range of high 10^{11} to low 10^{13} m^{-3}, and electron temperatures on the order of 0.5-1 eV (eV=11604 ^{o}K) were produced in the vacuum chambers. With the plasma source off the chamber pressure was about $5x10^{-7}$ Torr. During the operation of the source the background pressure was in the high 10^{-5} to low 10^{-4} Torr. Various diagnostics were used to determine the plasma conditions around the array segments, which are described in greater detail in Jongeward, G. *et al*.7

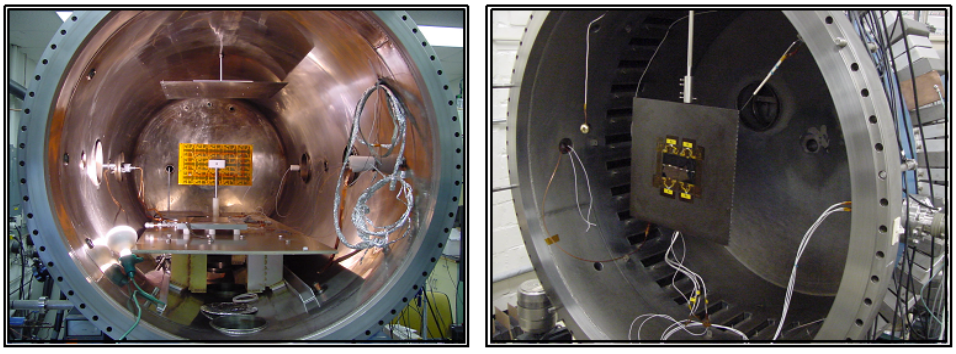

Figure 4. The ISS and TECSTAR coupon setups in the NASA MSFC vacuum chambers.

Summary of Results From Experiments and Modeling

Electron collection experiments

Electron collection measurements were performed in both vacuum chambers. Only one coupon was tested each time in the chamber. All solar cells on each coupon were positively biased (at the same voltage) with respect to ground. Current collection measurements were obtained for the applied voltage range 200-500 V.

The data reveal two main trends for the ISS coupons: (a) relaxation time is in the order of tens to hundreds of seconds. Figure 5 shows representative signals collected during the period 9/5-11, 2002 using the original coupon, dubbed "ISS-A." (b) The variability (standard deviation divided by the mean value) of collected current after exposure to the plasma for 300 seconds generally increases with bias voltage, ranging 13-27% for ISS-A and 26-71% for the second ISS coupon tested, the "ISS-B." ISS-B also collected higher currents the longer the coupon was tested (Figure 6, left). Similarly to the ISS coupons, the TECSTAR sample also exhibited large variability at each bias voltage, as shown in Figure 6, right. However, in contrast to ISS the variability generally decreased with increasing bias voltage, from 43% (at 300 V) to 18% (at 500 V). Table 1 lists average values of electron current collection after 300 seconds, scaled to nominal plasma density of 10^{13} m^{-3} and electron temperature of 0.55 eV. The scaled values were used to determine the variability of the measurements at each bias voltage.

Table 1. Average electron current collected by ISS and TECSTAR coupons (after 300 sec) at j_{th}=200 mA/m^2. Coupon collecting areas: A_{ISS}≈9.75e-4m^2 (ISS), A_{TEC} ≈ 2.07e-4 m^2 (TECSTAR).

Applied Voltage (V)	ISS-A Avg. I (mA)	ISS-B Avg. I (mA)	TECSTAR Avg. I (mA)	TECSTAR (xA_{ISS}/A_{TEC}) Avg. I (mA)
200	2.038	0.407	0.055	0.233
300	5.538	1.201	0.180	0.776
400	10.31	2.687	0.405	1.745
500	16.88	5.974	0.661	2.875

Dynamical effects due to dielectric charging during electron collection were determined to be negligible under the conditions of the experiments.[13] In the absence of charging effects other mechanisms that may possibly lead to the prolonged times observed during current collection must be considered. For example, it is possible that the high electron fluxes and energies bombarding the dielectrics at these high voltages may alter the materials' secondary electron yield (SEY) properties. There have been numerous studies on the adverse effects of "electron-clouds" on high-energy particle accelerator facilities that involved measurements of the change in secondary electron yield (SEY) properties with charged-particle dose (in units of charge per unit area) for various metals.[14,15] These efforts were primarily motivated by the need to reduce the electron cloud generated by secondary electron emission of metal surfaces. One proposed way to reduce this effect has in fact been to condition the emitting surface, by exposing it to electron doses that are sufficiently high to permanently reduce its secondary electron yield

characteristics. The results from one such study on copper is reported by Baglin, I., *et al*.[15] Recent modeling work has also suggested that changing SEY material properties may indeed be a driving mechanism for the observed current collection trends.[13] However, both the lack of SEY measurements for the dielectric material on the ISS coupons, and the significant variability in current collection observed during the tests, do not allow for a conclusive assessment based on the comparisons made between theory and experiment.

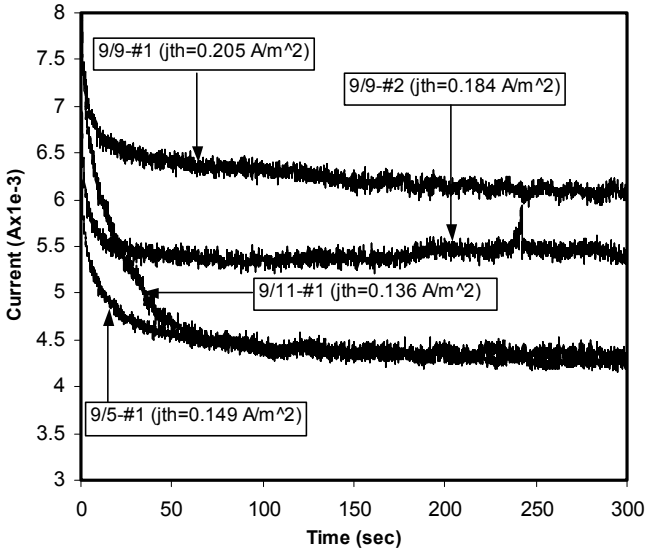

Figure 5. Representative transient data for the ISS-A coupon biased to 300 Volts.

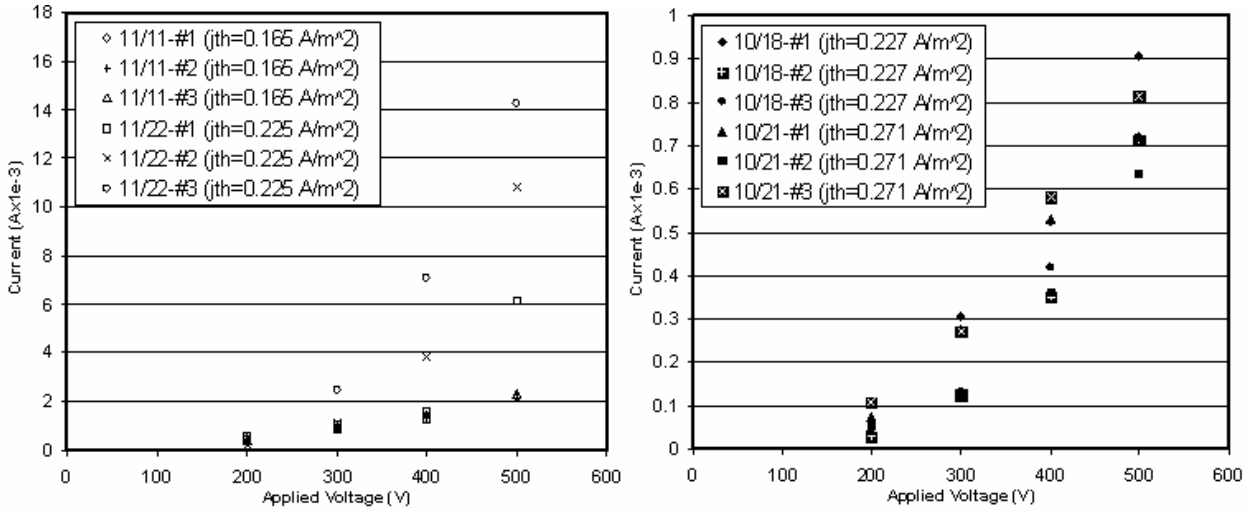

Figure 6. Left: Electron current collected by the ISS-B coupon, after 300 sec, on various days during the 11/2002 tests. Right: Electron current collected by the TECSTAR coupon, after 300 sec, on various days during the 10/2002 tests.

Experiments to determine arcing thresholds

We present here a summary of results from tests during which the coupons were biased negatively with respect to the plasma. The electrical circuits, setups and assessments of arc discharge initiation and coupon damage that occurred during these tests are described in greater detail by Schneider, T. *et al.*[16] The ultimate goal of the experiments was to define operating limits for the D2HET array below which the possibility of damage from sustained arcs would be minimized if not completely eliminated. These limits or "thresholds" would in turn guide the design of the solar array, specifically in regards to the maximum potential difference that would be allowed between adjacent solar cells.

The results from the sustained arc tests are shown in Figure 7. Figure 7, left provides threshold values in terms of power in the arc, sustained current and voltage drop across those ISS cells that supported the arc. The TECSTAR results are shown in Figure 7, right. The red-circled points in Figure 7, right are first-time occurrences, i.e. the recorded values were obtained only the first time the case was performed. Subsequent runs of the same cases yielded different values that, in most cases, were more consistent with each other.

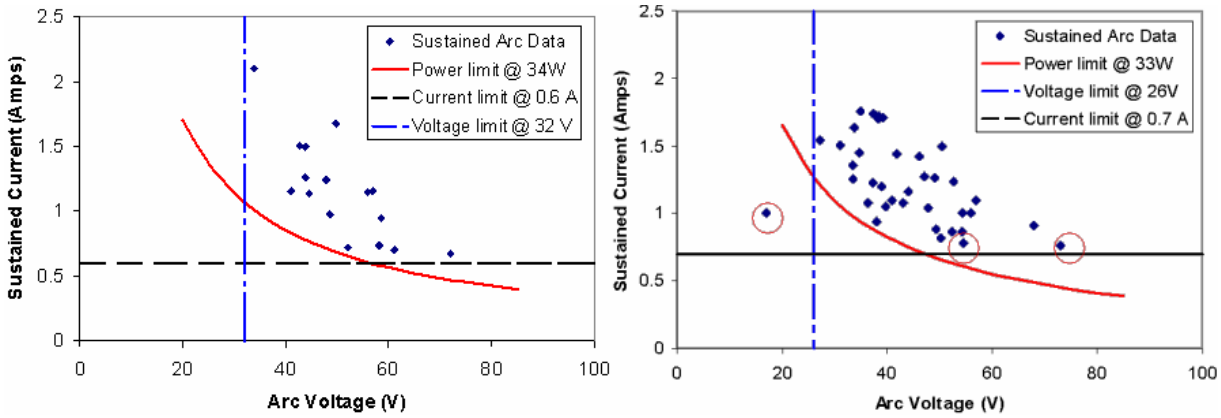

Figure 7. Left: Sustained arc thresholds for ISS design. Right: Sustained arc thresholds for TECSTAR (planar) design.

D2HET Solar Array Design

The test results above suggest both high electron collection and low arcing thresholds. The first would lead to degradation of the array performance if not taken into account in the design. If adjacent cells are not designed to operate below the sustained-arcing threshold then arcs may lead to permanent damage of the array.

A design approach is followed here that reduces inefficiencies by electron collection, allows a maximum differential voltage at about the observed arc voltage threshold between cells while providing additional security against sustained arcing. Specifically, the design employs coverglass sheets that cover more than one cell thus reducing the number of cell sides that can collect electrons. The design also arranges strings (of in-series cells) such that the maximum voltage difference between two cells is approximately equal to the measured arc voltage threshold. Additional security against arcs is implemented by organizing coverglass sheets in an

alternating manner such that the plasma expelled during trigger arcs, which can lead to sustained arcs, is partially blocked from reaching those adjacent cells that are at the highest potential difference. We also arrange strings in a manner that reduces induced torques with the ambient magnetic field.

Based on the electron collection tests, the TECSTAR technology is used as the basis for the D2HET array. As shown in Table 1, at 300 V the TECSTAR coupon collected about 1.5 times less current than ISS-B. Both the lower performance of the ISS cells and the large differences in collected current observed between "identical" coupons make it a less favorable technology compared to TECSTAR.

Solar cell performance

For the design the solar cell performance parameters listed in equation (1) are assumed,[17] where V_{mp}, i_{mp} and P_{mp} are the cell voltage, current and power at the optimum power output point.

$$\begin{aligned} &V_{mp} = 2.29\,\mathrm{V} \\ &i_{mp} = 0.445\,\mathrm{A}\ (j_{mp} = 158.4\,\mathrm{A/m^2}\ \text{for}\ 37\mathrm{mm\,x\,76mm\,cell}) \\ &P_{mp} = 1.02\,\mathrm{W} \end{aligned} \tag{1}$$

The cell type and size are very similar to the original TECSTAR coupon (Figure 3). From Table 1 and the TECSTAR coupon geometry the following empirical relationship are deduced for the non-dimensional electron current density collected, $\bar{j}_{ec}$:

$$\begin{aligned} &\chi \equiv \frac{eV}{kT_e},\ \ \bar{j}_{ec} \equiv \frac{j_{ec}}{j_{e,th}} = c_1 \chi^{c_2} \\ &c_1 = 6.495\mathrm{x}10^{-7},\ \ c_2 = 2.5 \end{aligned} \tag{2}$$

where $j_{e,th}$ is the electron thermal current density, e is the electron charge, V is the cell voltage, k is the Boltmann factor and T_e is the electron temperature. The fitting constants are c_1 and c_2. The following nominal conditions were used to deduce equation (2) above (which is also plotted in Figure 8 below): $j_{e,th}$ = 200 mA/m^2, V = 200-500 volts, T_e = 0.55 electronvolts.

With A_c being the collecting area, the current collected per cell i_{ec} may then be expressed as,

$$i_{ec} = \bar{j}_{ec} j_{e,th} A_c = c_1 \chi^{c_2} j_{e,th} A_c \tag{3}$$

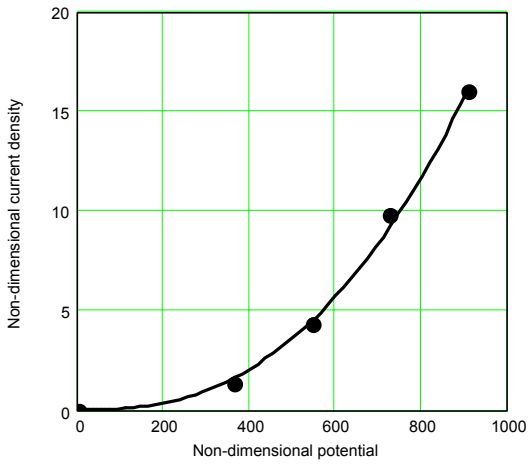

Figure 8. Empirically-reduced dependence of non-dimensional electron collection $\bar{j}_{ec}$ on the non-dimensional collection potential χ, based on averaged data from the TECSTAR coupon tests.

The design approach presented here provides additional security against arcing that can be sustained between cells. It also improves the electron collection current ratio η_{ec}, defined by equation (4) below, where, I_{ec} is the total electron current collected and I_o is the total operating current.

$$\eta_{ec} \equiv \frac{I_{ec}}{I_o} \tag{4}$$

A modified arrangement of the TECSTAR sample coupon in regards to the coverglass is proposed. Specifically, the coverglass sheet is placed to cover more than one cell thus shielding some of the exposed cell sides from collecting electrons. The solar cell size is similar to the original TECSTAR cell tested at NASA MSFC (Figure 3): t = 6.1 mil, Lc= 37 mm, Wc= 76 mm, where, t is the cell thickness, Lc is the cell length (taken here as the short side of the cell) and Wc is the cell width (taken here as the long side of the cell).

Solar array for low-power deep space mission

A design that is based on the Deep Space-1 (DS-1) spacecraft power requirement is presented in this section. In a subsequent section all pertinent parameters are re-computed to produce a design for a higher power spacecraft. The power requirements are comparable to those specified by NASA in a recent Design Reference Mission (DRM) that was part of an NASA Research Announcement (NRA) solicitation (http://www.spacetransportation.com/code_s/AdvancedSEP.pdf). The DRM required solar arrays capable of providing a total of 30 kW, and solicited component and subsystem development of Solar Electric Propulsion (SEP) technologies that have the potential to provide benefits beyond those provided by Ion propulsion.

DS-1 operated the NASA Solar Electric Propulsion Technology Applications Readiness (NSTAR) ion engine,[18] which required a maximum power of about 2.1 kW. The solar arrays

produced a maximum of 2.5 kW.[19] A recent calculation to estimate the mass benefits from direct-drive drive compared specifically the DS-1 NSTAR conventional system and the same type of spacecraft and mission requirement using a D2SPT-100. The results from that comparison were favorable for the D2SPT-100 in that it reduced the total launch mass by 4%.[20] A similar DS-1 type of spacecraft, with a total power capability of 2.25 kW is therefore chosen here, as a representative low-power mission on which to base the design of the solar array. The spacecraft is assumed to employ a single SPT-100 (requiring about 1.5 kW of power) for primary propulsion, operating in direct drive mode.

The strings are designed to produce a voltage of V_o=316 V. Thus, the number of cells in series N_s must be,

$$N_s = \frac{V_o}{V_{mp}} = \frac{316}{2.29} = 138 \tag{5}$$

For a total power requirement of P_o=2.25 kW we must have,

$$N_t = \frac{P_o}{P_{mp}} = \frac{2252}{1.02} = 2208 \rightarrow N_p = \frac{N_t}{N_s} = \frac{2208}{138} = 16 \tag{6}$$

where, N_t is the total number of cells, N_p is the number of cells in parallel.

Cell arrangement and array size. The proposed solar array arrangement is shown in Figure **9**. The arrangement minimizes torques that may be induced by the interaction of solar array currents and the ambient magnetic field, and ensures no more than V_{arc} = 27.5 V differential between adjacent cells.

From V_{mp} = 2.29 V the number of cells in each row of a single string $N_{s,row}$ is computed as,

$$N_{s,row} = \frac{V_{arc}}{2V_{mp}} = 6 \tag{7}$$

Then the width of each 6-cell row in a string (and therefore the width of each string) w_{row} is approximately

$$w_{row} \approx N_{s,row} Lc = 0.22\,\text{m} \tag{8}$$

If the two strings are united into one submodule (as shown in Figure 9 top) then the

- submodule would produce $2i_{mp}$=0.89 A and $2N_sV_{mp}i_{mp}$ = 0.282 kW
- number of submodules required would be $N_t/N_s/2$ = 8 submodules (4 on each side of the spacecraft bus)
- approximate width of the submodule would be $2w_{row} \approx$ 0.44 m
- approximate array width on each side of the spacecraft bus would be $W_{SA} \approx 4w_{row}$ = 0.88 m.

- approximate length of the array on each side of the spacecraft bus would be $L_{SA} \approx 2[N_s/N_{s,row}]Wc = 3.5$ m.

A summary of the proposed array design parameters is provided in Table 3.

Coverglass arrangement and η_{ec}. Using equation (3) the total collection current by the solar array may be estimated by summing up the collection by each cell as shown in equation (9),

$$I_{ec} \approx c_1 j_{e,th} A_c N_p \sum_{n=0}^{N_s-1} \chi_n{}^{c_2}$$
$$\chi_n = \frac{e\phi_n}{kT_e},\ \phi_n \equiv \frac{2n+1}{2} V_{mp} \tag{9}$$

where it is assumed that each cell is collecting at an effective potential of ϕ_n.

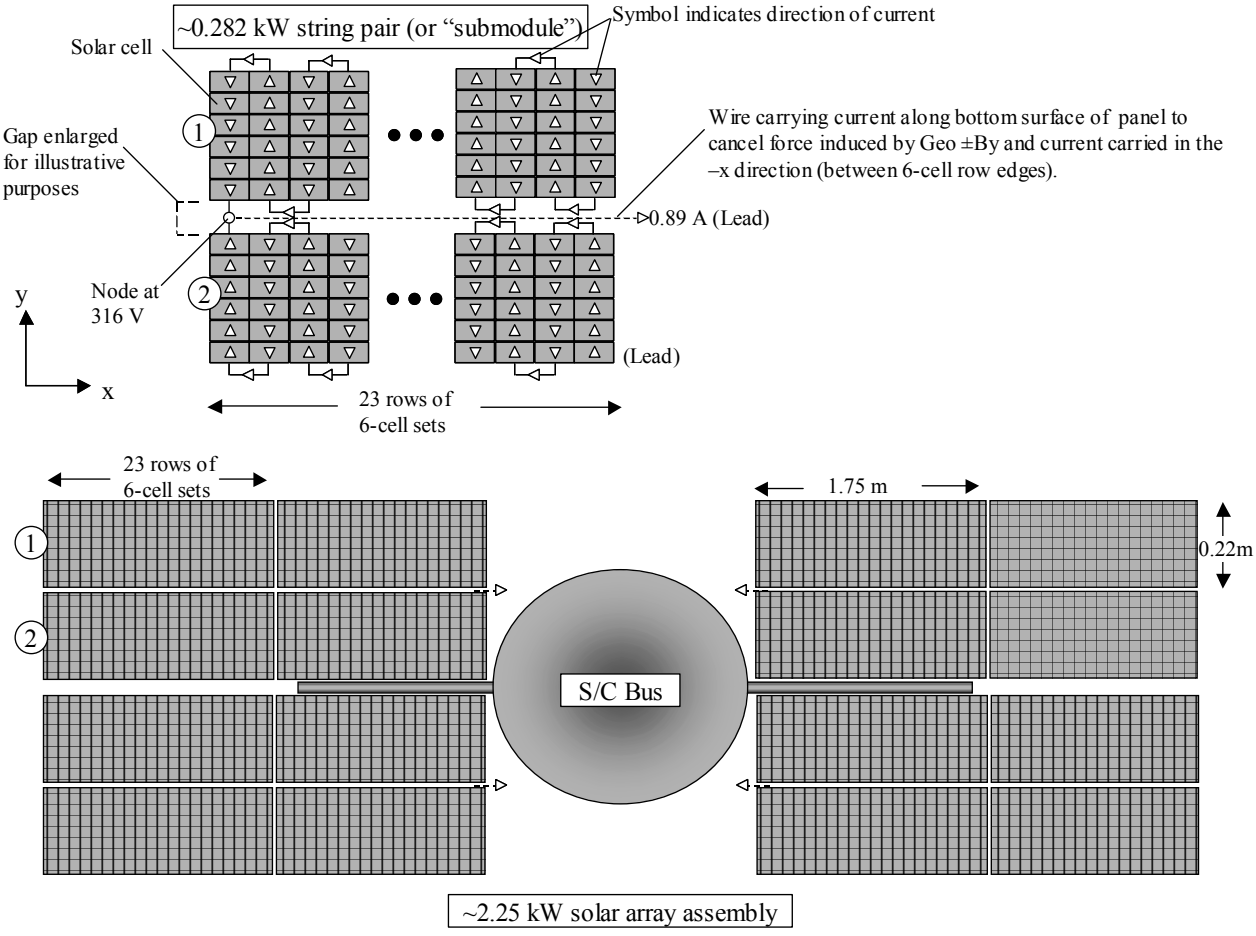

Figure 9. Arrangement of panels in a proposed design of a 2.25 kW D2HET solar array. The design is based on a DS-1 type of spacecraft and mission that would operate a single SPT-100 in direct drive mode.

For the design shown in Figure 9, assuming that all four sides of each cell are exposed and therefore allowed to collect (i.e. $A_c=2t(Lc+Wc)$), η_{ec} is approximated as follows:

$$\eta_{ec} \approx \frac{c_1 j_{e,th} A_c \sum_{n=0}^{N_s-1} \chi_n^{\,c_2}}{i_{mp}} = 3.17\text{x}10^{-3} \qquad (10)$$

It is noted that the result of equation (10) is for a thermal electron current of 200 mA/m^2 (based on a plasma density of n=10^7/cc and temperature of Te=0.55 eV). Table 2 illustrates the range of values η_{ec} may acquire if no measures are taken to cover part or all of the exposed cell areas that may collect electrons. To account for the higher plasma densities that may be present (e.g. see Figure 1), which is strongly dependent upon mission, spacecraft configuration, thruster position relative to arrays, etc., and to reduce even further the possibility of arcing across those cells that are at the maximum potential difference of 27.5 V, the alternating coverglass arrangement shown in Figure 10 is proposed. The design in Figure 10 would require 22 sheets of Coverglass-A size and 2 sheets of Coverglass-B size, per string. Another option would be to cover 2x2 cells (instead of 2x3).

Table 2. Approximate changes in η_{ec} with various plasma conditions attainable in the plume of an HET.

	$n_e = 10^{12}$ m^{-3}		$n_e = 10^{13}$ m^{-3}		$n_e = 10^{14}$ m^{-3}	
Te	$j_{e,th}$ (mA/m^2)	% η_{ec}	$j_{e,th}$ (mA/m^2)	% η_{ec}	$j_{e,th}$ (mA/m^2)	% η_{ec}
0.1	8.48	1	84.8	10	848	100
1	26.8	10^{-2}	268	10^{-1}	2680	1
10	84.8	10^{-4}	848	10^{-3}	8476	10^{-2}

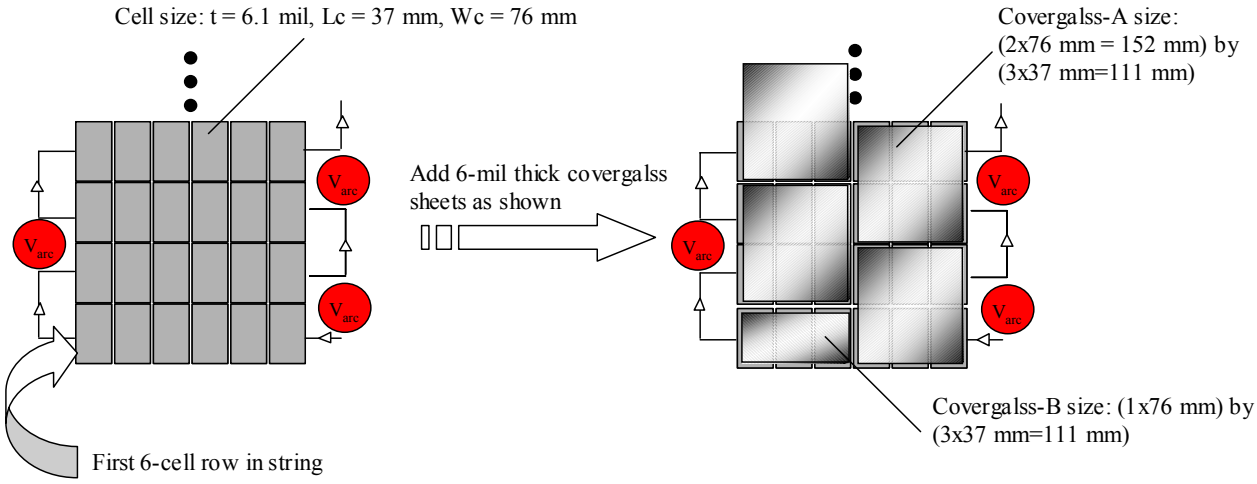

Figure 10. Proposed covergalss arrangement on a solar array string with V_{arc}=27.5 V.

Solar array for high-power deep space mission

The approach outlined above is applied to design a solar array for a total power requirement of 30 kW. The power level is chosen based on a recent NASA DRM (http://www.spacetransportation.com/code_s/AdvancedSEP.pdf). Such power levels may be used to operate Hall propulsion at tens of kilowatts. One example of a potential thruster candidate is the NASA GRC 50-kW class 457 M operated at lower than nominal powers (which has already been demonstrated at GRC),[21,22] or two BPT-4000 engines requiring a total of ~8 kW. We recognize that the plasma conditions generated by these higher-power propulsion systems may differ drastically from the nominal conditions emulated in the laboratory during the D2HET program (which were based an a specific 2x2 spacecraft-thruster matrix). Therefore, as suggested by Table 2, the proposed design may not sufficiently minimize electron collection and/or arcing. The advantages of the design would be heavily dependent upon spacecraft geometry, thruster location relative to the arrays, and of course the type of thruster.

The solar array design parameters are re-computed for two maximum operating voltages, 300 V and 500 V. The results are summarized in Table 3.

Table 3. Summary of direct drive solar array design parameters for different S/C requirements.

Sol. Array parameter	300-V solar array for low-power spacecraft	300-V solar array for high-power spacecraft	500-V solar array for high-power spacecraft
Cell size	Lc=37 mm, Wc= 76 mm t = 6.1 mil	Lc=37 mm, Wc= 76 mm t = 6.1 mil	Lc=37 mm, Wc= 76 mm t = 6.1 mil
P_o	2.25 kW	36.035 kW	33.195 kW
V_{max}	316.1 V	316.1 V	517.54 V
I_o	7.12 A	113.9 A	64.1 A
η_{ec} (max[§])	0.317%	0.317%	1.78%
N_s	138	138	226
N_t	2208	35328	32544
N_p	16	256	144
$N_{s,row}$	6	6	6
w_{row}	0.22 m	0.22 m	0.22 m
$N_t/N_s/2$	8 submdls (4 on each side of S/C in 2x2 setup)	128 submdls (64 on each S/C side in a 8x8 setup)	72 submdls (36 on each S/C side in a 6x6 setup)
$2i_{mp}$	0.89 A	0.89 A	0.89 A
$2N_sV_{mp}i_{mp}$	0.2815 kW	0.2815 kW	0.461 kW
W_{SA}	0.88 m	3.55 m	2.66 m
L_{SA}	3.5 m	13.97 m	17.164 m

[§]Assumes all cells collect electrons and therefore the actual value will be reduced with the proposed coverglass arrangements. The precise reduction would depend on the specific coverglass arrangement.

Summary and Conclusions

Two solar array technologies have been tested for electron current collection at voltages in the range 0-500 V, as part of a program sponsored by NASA to develop a Direct Drive Hall Effect Thruster system. The first technology sample was a coupon containing (3x5), single-junction silicon cells that are almost identical to those used onboard ISS, and thus have no exposed interconnects. The second coupon was a Solar Power Module designed by TECSTAR (now part of EMCORE Corp.) that utilizes multi-junction cells with conventional interconnects. Both coupons exhibited transient variations in current collection with characteristic times greatly exceeding dielectric charging times. After many hours of exposure to the plasma the first of two 3x5 coupons, ISS-A, cut from the same 80-cell PPM at NASA GRC, collected 2-5 times more current than its counterpart did, ISS-B, when it was first tested at NASA MSFC. ISS-B exhibited increased current collection with increasing exposure to the plasma. TECSTAR also displayed transient collection. All coupons showed large variability from the mean value. For ISS the variability increased with bias voltage; for TECSTAR it decreased. Combined with results from electron collection modeling, and from experiments at negative applied voltages (ion collection) that determined arcing thresholds for the two technologies, the observations have allowed for a preliminary design of a low-power (~2 kW) and higher power D2HET solar arrays.

Acknowledgments

This work was supported under NASA Glenn Research Center contract NAS3-01100.

References

[1] Oleson, S.R., "Electric Propulsion for Low Earth Orbit Communications Satellites," IEPC paper 97-102, Aug. 1997.

[2] Oleson, S.R., Myers, R.M., "Advanced Propulsion for Geostationary Orbit Insertion and North-South Station Keeping," J. of Spacecraft and Rockets, Vol. 34, No. 1, pp. 22-28, Jan-Feb 1997.

[3] Oleson, S.R. and Sankovic, J.M., "Advanced Hall Electric Propulsion for Future In-Space Transportation," NASA TM-2001-210676, April 2001.

[4] Hamley, J.A., et al., "Hall Thruster Direct Drive Demonstration," AIAA-97-2787, July 1997.

[5] Kerslake, T.W., and Gefert, L.P., "Solar Power System Analyses for Electric Propulsion Missions," NASA/TM-1999-209289, July 1999.

[6] Dudenhoefer, J.E., and George, P.J., "Space Solar Satellite Technology Development at the Glenn Research Center – An Overview," NASA/TM-2000-210210, July 2000.

[7] Jongeward, G.A., et al., " Development of a Direct Drive Hall Effect Thruster System," Society of Automotive Eng. (SAE), Power Systems Conference, Paper 02PSC-77, Oct. 2002.

[8] Hoskins, A., et al., "Direct Drive Hall Thruster System Development," AIAA-03-4726, July 2003.

[9] Kerslake, T.W., "Effect of Voltage Level on Power System Design for Solar Electric Propulsion Missions," ISEC Paper 2003-44008, March 2003.

[10] Katz, I., Davis, V.A., and Snyder, D.B., "Mechanism For Spacecraft Charging Initiated Destruction of Solar Arrays in GEO," AIAA-98-1002, Jan. 1998.

[11] Jongeward, G. A., et al., "The Role Of Unneutralized Surface Ions In Negative Potential Arcing," IEEE Trans. Nucl. Sci., 32, p. 4087, 1985.

[12] http://www.nrel.gov/ncpv/higheff.html

[13] Mikellides, I.G., et al., "Assessment of High-Voltage Solar Array Concepts for a Direct Drive Hall Effect Thruster System," AIAA-03-4725, July 2003.

[14] Kirby, R.E., et al., "Secondary Electron Emission Yields From PEP-II Accelerator Materials," SLAC-PUB-8212, Oct. 2000.

[15] Baglin, I., et al., "The Secondary Electron Yield of Technical Materials and its Variation with Surface Treatments," Proceedings of EPAC, p. 217, Vienna, Austria, 2000.

[16] Schneider, T., et al., "Experimental Investigation of Plasma Interactions with Candidate Solar Array Technologies for a Direct Drive Hall Thruster System," AIAA-03-5017, July 2003.

[17] Conversations with solar array manufacturers from EMCORE Corporation.

[18] Polk, J.E., et al., "Validation of the NSTAR Ion Propulsion System on the Deep Space One Mission: Overview and Initial Results," AIAA-99-2274, June 1999.

[19] http://nmp.jpl.nasa.gov/ds1/quick_facts.html

[20] Jongeward, G.A., et al., " Development of a Direct Drive Hall Effect Thruster System," NRA Review Presentation for the Enabling Concepts and Technologies Program at NASA GRC, Jan. 2003, SAIC Quarterly Report no. 03/2019.

[21] Jankovsky, R.S., Jacobson, D.T., Pinero, L.R., Sarmiento, C.J., "NASA's Hall Thruster Program 2002," AIAA-02-3675, July 2002.

[22] Manzella, D., Jankovsky, R., and Hofer, R., "Laboratory Model 50 kW Hall Thruster," AIAA-02-3676, July 2002.